crease at longer radical lifetimes was interpreted to mean that isomerizations leading to acyl radicals are irreversible.

Acknowledgment. We thank Mr. Donald Harvan of the National Institute of Environmental Health Sciences, Research Triangle Park, North Carolina, for his able assistance in obtaining the mass spectral data.

Registry No. **1a**, 3384-35-8; **2a**, 1785-68-8; **2b**, 117439-41-5; **3**, 1518-16-7; cyclohexyl methanesulfonate, 16156-56-2.

^{125}Te Solid-State NMR Spectra and Secondary Bonding Arrangements for Some Salts of the Trimethyltelluronium and Triphenyltelluronium Cations†

Michael J. Collins,*[1a,b] John A. Ripmeester,*[1a] and Jeffery F. Sawyer*[1c]

Contribution from the Division of Chemistry, National Research Council of Canada, Ottawa, Ontario K1A 0R9, Canada, and Department of Chemistry, University of Toronto, 80 St. George Street, Toronto, Ontario M5S 1A1, Canada. *Received September 28, 1987*

Abstract: The preparation of several salts of the Me_3Te^+ and Ph_3Te^+ cations is reported along with ^{125}Te static and CP/MAS solid-state NMR spectra of the Me_3Te^+ salts and ^{125}Te CP/MAS spectra of the Ph_3Te^+ salts. In addition, crystal structures of the salts $Me_3Te^+Cl^-\cdot H_2O$ (**1**), $Me_3Te^+I^-$ (**2**), $Me_3Te^+NO_3^-$ (**3**), $Ph_3Te^+NO_3^-$ (**4**), $Ph_3Te^+Cl^-\cdot{}^1/_2CHCl_3$ (**5**), and $(Ph_3Te)_2SO_4\cdot 5H_2O$ (**6**) have been determined to help in the interpretation of some of the above spectra. It is shown that secondary bonding interactions with the anions have significant and substantial influence on the geometries of the cations and their crystal packings and on the resulting NMR spectra in terms of the tellurium shielding tensors and isotropic chemical shifts and in the presence of long-range spin $^1/_2$ to spin $^3/_2$ couplings. These couplings are indicative of long-range covalent interactions between the anions and cations in this series of compounds. In particular, the ^{125}Te CP/MAS spectrum of $Me_3Te^+Cl^-\cdot H_2O$ consists of a septet due to coupling to two equivalent chlorine atoms. In the case of **4** and **5** the presence of 4 and 2 crystallographically independent Te atoms is confirmed in the NMR spectra. Crystal data for each compound: **1**, orthorhombic, space group *Pbcm*, a = 6.432 (1) Å, b = 11.413 (2) Å, c = 10.070 (2) Å; **2**, monoclinic, space group $P2_1/n$, a = 7.115 (1) Å, b = 9.673 (2) Å, c = 11.324 (3) Å, β = 107.72 (2)°; **3**, monoclinic, space group $P2_1/n$, a = 6.862 (2) Å, b = 11.105 (1) Å, c = 9.608 (1) Å, β = 94.96 (2)°; **4**, triclinic, space group $P\bar{1}$, a = 12.368 (2) Å, b = 14.755 (2) Å, c = 19.573 (3) Å, α = 84.54 (1)°, β = 72.37 (1)°, γ = 76.77 (1)°; **5**, triclinic, space group $P\bar{1}$, a = 11.813 (1) Å, b = 12.909 (1) Å, c = 13.167 (2) Å, α = 77.91 (1)°, β = 66.86 (1)°, γ = 82.18 (1)°; and **6**, monoclinic, space group $P2_1/n$, a = 11.495 (4) Å, b = 24.730 (5) Å, c = 25.386 (5) Å, β = 94.21 (3)°.

A large number of triorganochalcogenium salts $R_3M^+X^-$ have been prepared and many of their structures have been determined.[2] In all cases the cation is trigonal pyramidal with a lone pair completing the tetrahedron, that is an AX_3E geometry. Virtually all of these structures contain weak directed interactions or secondary bonds[3] between the chalcogen atoms and atoms in the anions. These secondary bonds, M···Y, are frequently considerably shorter than the sum of the van der Waals radii of the interacting atoms[4] and form roughly opposite the primary bonds to give AX_3YE, AX_3Y_2E, or, most commonly, AX_3Y_3E geometries. Some evidence for the charge transfer involved in these interactions has been claimed in deformation density maps for Me_2TeCl_2 (an $AX_4Y'_2E$ geometry).[5] Secondary bonding in structures containing the related MX_3^+ cations (M = S, Se, or Te; X = F, Cl, Br, or I) has recently been reviewed.[6]

The acquisition of nuclear magnetic resonance spectra of solids has become increasingly facile in recent years with the development of techniques such as cross-polarization (CP) and magic-angle spinning (MAS).[7] It was hoped that the solid-state ^{125}Te NMR spectra of some R_3Te^+ salts could be obtained and that these spectra would reflect changes in the secondary bonding environments of the Te nuclei. Compounds of the Me_3Te^+ cation were examined first since methyl group rotation usually provides efficient ^{1}H relaxation and therefore short recycle times in the ^{125}Te CP experiment. A preliminary communication describing the acquisition of some solid-state ^{125}Te NMR spectra has already appeared.[8]

† NRCC No. 28800.

Experimental Section

Materials. Me_3TeI was prepared by addition of a slight excess of MeI to Me_2Te (Strem) in CCl_4 solution followed by filtration of the white solid product; Me_3TeBr by distilling an excess of MeBr (Matheson) onto neat Me_2Te and evaporating off the excess MeBr from the resulting white powder; Me_3TeCl by stirring an aqueous solution of Me_3TeI with a n excess of AgCl powder for 1 h, filtering the AgCl/AgI residue, and evaporating the solvent; and Me_3TeNO_3 by mixing stoichiometric aqueous solutions of Me_3TeI and $AgNO_3$, filtering the AgI precipitate, and evaporating the solvent. Crystals of Me_3TeI and $Me_3TeCl\cdot H_2O$ were obtained by slow evaporation of aqueous solutions and Me_3TeNO_3 was obtained by slow evaporation of an CH_3CN solution. Crystals of $Ph_3TeCl\cdot{}^1/_2CHCl_3$ suitable for X-ray diffraction were prepared by dissolving Ph_3TeCl (Organometallics) in $CHCl_3$ and slowly evaporating the solvent, and Ph_3TeNO_3 was prepared by mixing stoichiometric aqueous solutions of Ph_3TeCl and $AgNO_3$, filtering off the AgCl precipitate, and slowly evaporating the solvent. $(Ph_3Te)_2Hg_2Cl_6$ was prepared as previously described.[9] Crystals of $(Ph_3Te)_2SO_4\cdot 5H_2O$ were prepared by

(1) (a) National Research Council. (b) Present Address: Sherritt Research Centre, Sherritt Gordon Mines Ltd., Fort Saskatchewan, Alberta, T8L 2P2 Canada. (c) University of Toronto.

(2) Ziolo, R. F.; Extine, M. *Inorg. Chem.* **1980**, *19*, 2964 and references therein.
(3) Alcock, N. W. *Adv. Inorg. Chem. Radiochem.* **1972**, *15*, 1.
(4) Bondi, A. *J. Phys. Chem.* **1964**, *68*, 441.
(5) Ziolo, R. F.; Troup, J. M. *J. Am. Chem. Soc.* **1983**, *105*, 229.
(6) Christian, B. H.; Collins, M. J.; Gillespie, R. J.; Sawyer, J. F. *Inorg. Chem.* **1986**, *25*, 777.
(7) Fyfe, C. A. *Solid State NMR for Chemists*; CFC Press: Guelph, Ontario, 1983.
(8) Collins, M. J.; Ripmeester, J. A.; Sawyer, J. F. *J. Am. Chem. Soc.* **1987**, *109*, 4113.
(9) Ponnuswamy, M. N.; Trotter, J. *Acta Crystallogr.* **1984**, *C40*, 1671.

0002-7863/88/1510-8583$01.50/0 Published 1988 by the American Chemical Society

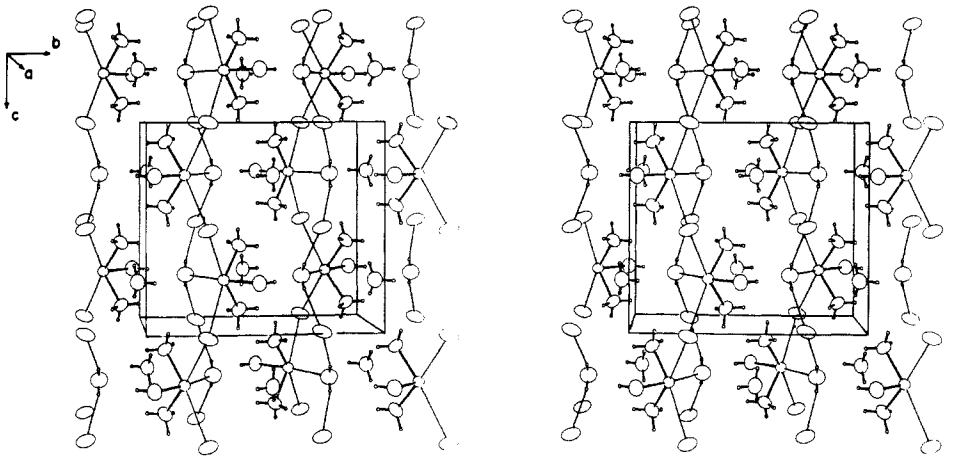

Figure 1. Crystal Packing in $Me_3Te^+Cl^-\cdot H_2O$ as viewed down *a*. Secondary bonds and hydrogen bonds indicated as thin lines.

mixing stoichiometric aqueous solutions of Ph_3TeCl and Ag_2SO_4 (Aldrich), filtering off the AgCl precipitate, slowly evaporating the solvent from the filtrate, and recrystallizing from ethanol.

NMR Spectroscopy. Tellurium-125 spectra were recorded at 56.8 MHz on a Bruker CXP-180 NMR spectrometer with a cross-polarization sequence. For the Me_3Te^+ compounds, static line shapes were typically recorded in 500 words of memory and zero-filled to 4 K, with a spectral width of 100 kHz, a cross-polarization contact time of 2 ms, and a delay time of 20 s. Magic-angle spinning was accomplished in Kel-F rotors of the Andrew-Beams type at approximately 3 kHz; spectra were generally accumulated in 1–4 K of memory and zero-filled to 8–16 K, with spectral widths of 20 kHz. The CP/MAS spectra of the Ph_3Te^+ compounds were recorded in 500 words of memory and zero-filled to 8 K with a spectral width of 100 kHz, a cross-polarization contact time of 10 ms, and a delay time of 20–30 s. All spectra were referenced to an external sample of neat Me_2Te. Telluric acid, $Te(OH)_6$, was used to set the cross-polarization conditions and as a secondary reference.[8] Carbon-13 CP/MAS spectra were recorded at 45.268 MHz on the same instrument, typically in 1 K of memory, and zero-filled to 4 K, with a spectral width of 20 kHz, a cross-polarization contact time of 3 ms, and a delay time of 4 s. Spectra were referenced to external neat TMS.

X-ray Crystallography. Crystals were sealed in 0.2–0.3 mm Lindemann capillaries as a precautionary measure against hydrolysis. Crystals of $Me_3Te^+I^-$ used in the X-ray studies were bright yellow (originally colorless), those of $(Ph_3Te)_2SO_4\cdot 5H_2O$ slightly yellow, and the others colorless or white, although it is noteable that the crystal of $Ph_3Te^+NO_3^-$ gradually turned light yellow during data collection. Cell and symmetry information were determined on an Enraf-Nonius CAD4 diffractometer with Mo Kα radiation (λ = 0.71069 Å) and are summarized in Table I (supplementary material) along with details of the intensity measurements and structure refinements. No systematic trends in the intensities of the standard reflections for **1–3** were observed; ca. 15%, 10%, and 23% declines in the intensities of the standard reflections for **4**, **5**, and **6** (Table I), supplementary material) were corrected for after data reduction. Lorentz and polarization corrections were applied to all data collected. Absorption corrections for **1–4** were made at a later stage in the refinements by the use of the program ABSORB of the Enraf-Nonius SDP package.[10] For compound **5** it was not possible to confidently identify crystal faces and in the case of **6** the regular shape and small absorption coefficient obviated any adsorption corrections. Averaging of equivalent data and the exclusion of systematically absent and zero F_{obs} data gave the final totals of independent reflections shown in Table I.

The positions of 4 Te atoms in $Ph_3Te^+NO_3^-$ were found with direct methods; otherwise, the positions of the heavy atoms were located by use of the Patterson function. Subsequent cycles of least-squares and Fourier calculations located all the remaining atoms. In **4** a 3:1 disorder in two of the oxygen atoms of the $N(3)O_3^-$ anion was observed. These disordered atoms were refined with isotropic thermal parameters only. Hydrogen atoms were located in ΔF Fourier maps or were placed in calculated positions (phenyl rings) with fixed temperature factors. For the Me_3Te^+ salts the positional parameters (and, in the case of **2**, the thermal parameters) of the H-atoms were allowed to refine in the final cycles of least-squares. Suitable weighting schemes and, where necessary, extinction corrections were applied and least-squares refinements then converged to the final residuals shown in Table I.

(10) *Enraf-Nonius Structure Determination Package*; B. A. Frenz and Associates: College Station, TX, 1981.

For all structures neutral atom scattering curves stored in the SDP program were originally taken from International Tables.[11] All computing was on a PDP 11/23 computer with programs in the SDP package.[10] The final atomic positional parameters for all structures are given in Table II (supplementary material).

Discussion of Crystal Structures

(1) $Me_3Te^+Cl^-\cdot H_2O$. The packing of this compound is the most regular of these reported here since it crystallizes in the orthorhombic space group *Pbcm* with the Me_3Te^+ cation and water of crystallization on crystallographic mirror planes and the Cl^- ion on a 2-fold axis. The hydrogen atoms of the water are out of the mirror plane so as to form hydrogen bonds to the Cl^- ion [Cl···H(1) = 2.44 (4) Å; O–H(1) = 0.79 (4) Å; Cl···H(1)–O = 166 (4)°; H(1)···Cl···H(1) = 112 (2)°], and one lone pair on oxygen in the mirror plane forms a secondary bond to tellurium [Te···O = 3.089 (4) Å; H–O···Te = 122 (3)°]. The AX_3Y_3E mono-capped octahedral environment of the Te is then completed by two Te···Cl secondary bonds [3.318 (1) Å (×2)] approximately trans to Te–C(1) [C(1)–Te···Cl = 172.14 (9)°, cf. C(2)–Te···O = 165.7 (2)°]. As a consequence the packing consists of infinite chains along *c* (Figure 1). Both the Te···Cl and Te···O contacts appear to be somewhat longer than analogous contacts, for example, in $Ph_3Te^+Cl^-$ (ref 2) and $Me_3Te^+NO_3^-$ below (Table III, supplementary material), although the present Te···Cl secondary bond lengths are significantly shorter than those observed in $Et_3Te^+Cl^-$ [3.448 (4) Å (×3)][12] and the majority of the contacts observed in a series of R_2TeCl_2 compounds containing edge-bridged $AX_4Y_2'E$ trigonal-bipyramidal Te atoms (Te···Cl ≥ 3.368 (4) Å, see Table III in ref 12). Furthermore, the Te···Cl and Te···O distances in the present salt are significantly shorter than corresponding Se···Cl and Se···O distances in several Ph_3Se^+ and Tol_3Se^+ salts,[13-15] with the exception of one contact in $(Tol_3Se)HSO_3$[15] (Table IV, supplementary material). Hydrogen bonding in these latter compounds is, however, generally stronger than that in $Me_3TeCl\cdot H_2O$ (Table V, supplementary material).

Presumably due to the unsymmetrical secondary bonded arrangement there is a significant difference in the CTeC bond angles of 96.1 (2)° and 93.9 (1)° (×2). In particular, the slightly stronger Te···Cl interactions (0.68 Å less than van der Waals distances) result in a small distortion in the overall geometry toward a square-pyramidal Me_3TeCl_2 arrangement with C(2) axial. Thus the cis and trans C–Te···Cl angles are closer to 90° and 180° than the corresponding C–Te···O angles [cis C–Te–O = 76.7 (1)° (×2); cis C–Te–Cl = 78.6 (1) [×2], 82.1 (1)°]. These CTeC bond angles are very close to the values reported for a

(11) *International Tables for X-ray Crystallography*; Kynock Press: Birmingham, U.K., 1965.
(12) Chadha, R. K.; Drake, J. E. *Can. J. Chem.* **1986**, *299*, 331.
(13) Mitcham, R. V.; Lee, B.; Mertes, K. B.; Ziolo, R. F.; *Inorg. Chem.* **1979**, *18*, 3498.
(14) Lee, J.-S.; Titus, D. D. *J. Cryst. Mol. Struct.* **1976**, *6*, 279.
(15) Bel'skii, V. K.; Bel'skaya, N. P.; Konyakhina, L. V.; Siskova, V. P. *Kristallografiya* **1982**, *27*, 1102.

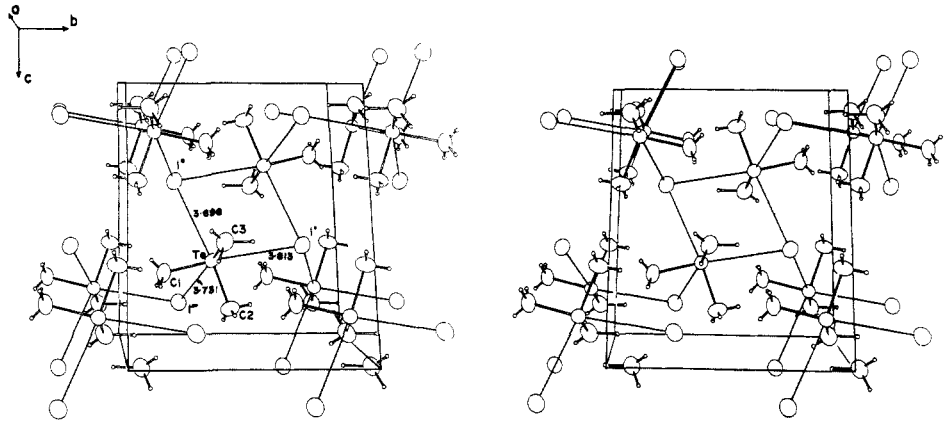

Figure 2. Crystal packing in $Me_3Te^+I^-$. Secondary bonds indicated as thin lines.

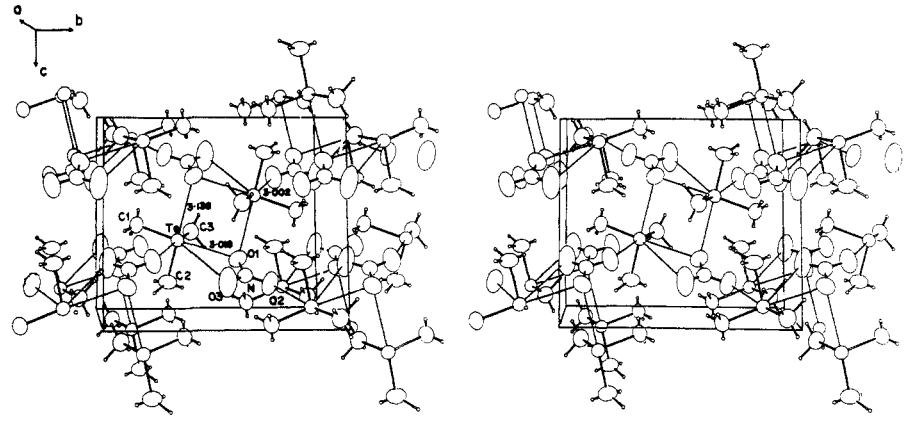

Figure 3. Crystal packing in $Me_3Te^+NO_3$. Secondary bonds indicated as thin lines.

(presumably) unsolvated form of Me_3TeCl[16] [where CTeC = 93.8, 94.1, and 95.7 (2)°] but are substantially larger than those observed in Et_3TeCl [85.8 (6)° (×3)][12] and Et_3TeBr [89.3 (6)°].[17]

(2) $Me_3Te^+I^-$. The AX_3Y_3E geometry of the Te atom in this compound is completed by 3 secondary Te···I contacts approximately trans to the Te–C bonds (Figure 2; Table III, supplementary material). These Te···I distances are 0.65, 0.62, and 0.54 Å less than neutral atom van der Waals distances.[4] Other Te···I secondary bond distances have been tabulated and discussed by McCullough, Knobler, and Ziolo.[18] These Te···I distances are ≥3.65 Å in length and the values in the present salt are fairly typical for Te···I secondary bonds and correspond to bond orders of 0.039, 0.035, and 0.027 with the Pauling equation[18] or bond valences of 0.138, 0.130, and 0.112 with an equation given by Krebs and Paulat.[19] It is noteable that in Et_3TeI[12] the CTeC bond angles are somewhat larger than those in Me_3TeI and the Te···I secondary bonding is weaker, with one of the interactions to complete the AX_3Y_3E geometry of Te even longer [4.494 (5) Å] than van der Waals distances (possibly due to disorder in one of the ethyl groups).

The angles I···Te···I (100.54, 105.77, and 115.23 (1)°) and Te···I···Te (74.23 (1), 98.38 (1), and 114.96 (2)°) indicate that there are no significant I···I contacts in the structure. Their presence would also lead to a much darker coloration for the crystals (cf. ref 20). The average CTeC angle in the iodide is virtually the same as that in the chloride above (94.2–94.3°).

(3) $Me_3Te^+NO_3^-$. The geometry of the Te atom in this cation is again AX_3Y_3E forming two short Te···O contacts to O(1) and one slightly longer contact to O(2) (Figure 3; Table III, supplementary material) which are 0.60, 0.59, and 0.46 Å less than van der Waals distances (bond valences:[21] 0.138, 0.135, and 0.113 Å). As a consequence of these interactions the bond N–O(1) [1.261 (4) Å] is significantly lengthened over N–O(2) and N–O(3) [1.200 (5) and 1.212 (5) Å].[22] Similar lengthening of a N–O bond as a consequence of charge-transfer interactions has been observed in $S_4N_3^+NO_3^-$ (by ca. 0.043 Å) where the charge transfer from the oxygen to the disulfide bond of the cation has been observed in difference-density maps.[23] Similarly, in $Ca(NO_3)_2 \cdot 3H_2O$ two types of nitrate coordination mode are observed among the eight crystallographically independent anions, and average N–O distances involving oxygen atoms forming two, one, and zero Ca^{2+}···O contacts were 1.267, 1.233, and 1.215 Å, respectively.[24] When directly bonded, however, the N–O bond length is ca. 1.33 Å (e.g., $Ph_2Te(NO_3)_2$, where Te–O = 2.171 (3) Å).[25] In $Ph_2Te(NO_3)_2$ four other face-capping Te···O contacts of lengths 2.904 (5) (×2) Å and 3.205 (5) (×2) Å are observed giving rise to an AX_4Y_4E geomery for the tellurium. In some related basic nitrates described in the same paper more complex overall geometries are observed with Te···O contacts in the range 2.862–3.514 Å,[25] and in two phenoxatellurin nitrates, Te···O distances are 3.096, 3.085, and 3.307 Å in an AX_4Y_3E geometry and 2.901 (×2) and 3.210 (×2) Å in an AX_4Y_4E geometry.[26] In several organo tellurium(IV) acetates, however, the secondary Te···O distances are all >2.95 Å in length.[27]

(16) Quoted in the discussion of the structure of Me_3TeBPh_4 (Ziolo, R. F.; Troup, J. M. *Inorg. Chem.* **1979**, *18*, 2271).
(17) Chadha, R. K.; Drake, J. E.; Khan, M. A.; Singh, G. J. *Organomet. Chem.* **1984**, *260*, 73.
(18) McCullough, J. D.; Knobler, C.; Ziolo, R. F. *Inorg. Chem.* **1985**, *24*, 1814.
(19) Krebs, B.; Paulat, V. *Acta Crystallogr.* **1976**, *B32*, 1470.
(20) McCullough, J. D. *Inorg. Chem.* **1975**, *14*, 1143.
(21) Brown, I. D. *J. Solid State Chem.* **1974**, *11*, 214.
(22) The O(1)–N–O(2), O(1)–N–O(3), and O(2)–N–O(3) bond angles are 119.8 (4), 119.8 (4), and 120.2 (4)°, respectively.
(23) Guru, Row, T. N.; Coppens, P. *Inorg. Chem.* **1978**, *17*, 1670.
(24) Leclaire, A. *Acta Crystallogr.* **1976**, *B32*, 235.
(25) Alcock, N. W.; Harrison, W. D. *J. Chem. Soc., Dalton Trans.* **1982**, 1421.
(26) Mangion, M. M.; Smith, M. R.; Meyers, E. A. *J. Heterocycl. Chem.* **1973**, *10*, 533 and 543.
(27) Bulgarevich, S. B.; Rivkin, B. B.; Furmanova, N. A.; Exner, O. O.; Movshovich, D. Y.; Yusman, T. A.; Sadekov, I. D.; Minkin, V. I. *Zh. Strukt. Khim.* **1984**, *25*, 97. Alcock, N. W.; Harrison, W. D.; Howes, C. *J. Chem. Soc., Dalton Trans.* **1984**, *1709*.

The overall crystal packing of Me_3TeNO_3 is very similar to that of Me_3TeI above (Figures 2 and 3). In both cases there are dimeric units about centers of symmetry that are linked by further secondary bonds in the [11$\bar{1}$] and [1$\bar{1}\bar{1}$] directions to give sheets approximately in the (101) plane.

(4) $Ph_3Te^+NO_3^-$. In this salt the four independent Te atoms each have slightly different primary and secondary bonding environments. This can be seen in Tables III and VI (supplementary material) where the number and lengths of the Te···O secondary bonds to each Te in the structure differ (due in part to disorder in the anion $N(3)O_3^-$) and in Table VII (supplementary material) in which the sum of the squared deviations in the CTeC angles from the mean values for Te(1) to Te(4) are indicated. The most regular environment is that of Te(3) [AX_3Y_3E with 3 Te···O secondary bonds of similar length], while the environments of Te(1), Te(2), and Te(4) are more complex (Table VI, supplementary material). In the case of Te(2) and Te(4) the secondary bonding is distorted by the close approach of adjacent phenyl rings [Te···C ≥ 3.63 Å] of other Ph_3Te^+ cations. These contacts should be compared to the van der Waals limit of ca. 3.76 Å, Te···Ph contacts ≥3.80 Å in $Ph_4Te\cdot{}^1/_6C_6H_6$,[28] and perhaps more significant contacts of ca. 3.4–3.5 Å in 1-methyl-3,4-dibenzo-1-telluracyclopentane and 1-phenyl-1-telluracyclopentane tetraphenylborate.[29] In addition to these Te···Ph contacts and the contacts in Table III (supplementary material), Te(1), Te(2), and Te(4) also form (with the exception of Te(2)···O(35) = 3.06 Å involving an atom from the disordered anion) several longer Te···O contacts ≥3.39 Å in length in directions that very approximately bridge C···E edges of the TeC_3E tetrahedra describing the primary geometry of each Te atom (Table VI, supplementary material). Noteably, N(4)–O(41) = 1.255 (6) Å and possibly the bonds to the disordered atoms O(34) and O(35) are the only substantially lengthened bonds and other N–O bond lengths in the nitrates are 1.191–1.234 (6) Å.

Overall the packing consists of two different centrosymmetric tetrameric units (Figures 4 and 5) that differ noteably only in slight changes in the relative orientations of the nitrate anions and phenyl rings (see below).

(5) $Ph_3Te^+Cl^-\cdot{}^1/_2CHCl_3$. As with $Ph_3Te^+NO_3^-$ and most Ph_3Te^+ salts, more than one independent Te environment is observed in that Te(1) forms an AX_3Y_3E arrangement with 3 Te···Cl contacts and Te(2) an AX_3Y_2E arrangement with 2 Te···Cl contacts (Table III, supplementary material). None of these chlorine atoms are from the solvent that is only weakly held in the lattice. One chloride ion thus interacts with three Te atoms and the other with two Te atoms about centers of symmetry to give the tetrameric step-like arrangement shown in Figure 6, where it is also apparent that the vacant secondary bond position on Te(2) is blocked by the phenyl group **13** on Te(1) (Te···C(135) = 3.672 (5) Å; Te···C(136) = 3.740 (4) Å). The $CHCl_3$ solvent then sits in cavities between these tetramers with an average C–Cl and Cl–C–Cl bond length and bond angle of 1.703 Å and 94.4°, respectively (Figure 7). A similar tetrameric unit has been observed for Ph_3TeNO_3 above, for the $Ph_3Te(NCS)$ unit in $[Ph_3Te(NCS)]_4[Ph_3Te(NCS)]_2$,[30] and for $Ph_3Te(NCO)\cdot{}^1/_2CHCl_3$,[31] where both ends of the NCS^- and NCO^- anions are involved in Te···N, Te···O, and Te···S secondary interactions.

As such the tetrameric unit is completely different from the packing arrangement in unsolvated $Ph_3Te^+Cl^-$ (ref 2) which is based on dimeric units. Two other solvated forms of $Ph_3Te^+Cl^-$ with $^1/_2(C_6H_6)$ and $^1/_2(Et_2O)$ in the lattice have been identified.[2] Although complete details have not been reported, preliminary results indicate that they do not contain dimeric units. This along with the triclinic unit cells suggest that tetrameric units are again likely. In comparing the unsolvated and solvated forms of

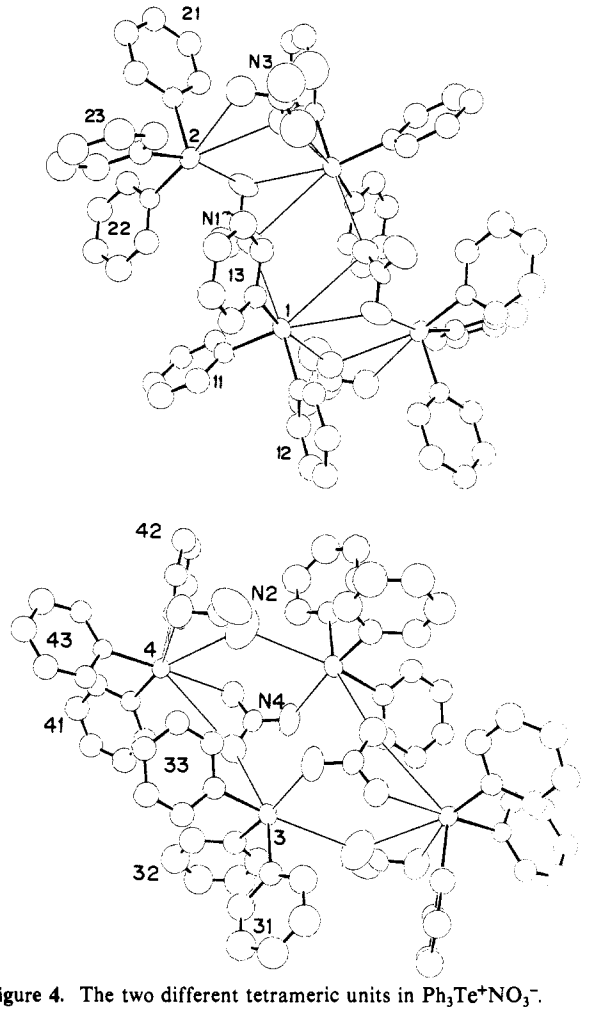

Figure 4. The two different tetrameric units in $Ph_3Te^+NO_3^-$.

$Ph_3Te^+Cl^-$ we can note that, notwithstanding the increase in the coordination number of Cl(1) in the present salt, Te···Cl interactions in the solvated form are longer and weaker than those in the unsolvated form (Table III, supplementary material).

(6) $(Ph_3Te)_2SO_4\cdot 5H_2O$. The asymmetric unit of this compound contains four Ph_3Te^+ cations, two sulfate anions, and ten water molecules linked by a complex network of Te···O secondary bonds (Table III, supplementary material) and hydrogen bonds (Table V, supplementary material) into infinite chains along *a* (Figure 8). Each Ph_3Te^+ cation has significantly different primary bond lengths and angles as shown by the asymmetry parameters in Table VII (supplementary material), although the average CTeC bond angle is the same for each cation.

For Te(1), the overall geometry may be described as AX_3Y_2E with two Te···O contacts to water molecules and the remaining A···Y secondary bonding direction blocked by phenyl ring **32** [Te(1)···H(324) = 3.51 Å]. Similarly, Te(2) forms two secondary bonds involving the oxygen atoms of two water molecules and a third to O(21) of a sulfate anion (AX_3Y_3E geometry), Te(3) has an $AX_3Y_3'E$ geometry involving oxygen atoms in three water molecules, and O(11) of the other sulfate anion and the geometry of Te(4) is AX_3Y_3E (Table III, supplementary material). The lengths of these Te···O secondary bonds vary significantly from 2.797 (9) Å up to the van der Waals limits. In general, the secondary bonding is stronger in the present salt than in either $(Me_3Te)NO_3$ or $(Ph_3Te)NO_3$ above and it is noteable that each Te forms one short (<2.94 Å) contact involving not oxygen atoms of the sulfate anions but water molecules instead. The sulfate anions appear to be more involved in hydrogen bonding with O···O contacts as short as 2.718 Å (Table V), supplementary material).

From Table IV (supplementary material) it is clear that the present Te···O distances are substantially shorter than the corresponding S···O contacts in the salt $(Me_3S)_2SO_4$.[32] Furthermore

(28) Smith, C. S.; Lee, J.-S.; Titus, D. D.; Ziolo, R. F. *Organometallics* **1982**, *1*, 350.
(29) Jones, R. H.; Hamor, T. A. *J. Organomet. Chem.* **1982**, *234*, 299.
(30) Lee, J.-S. Titus, D. D.; Ziolo, R. F. *Inorg. Chem.* **1977**, *16*, 2487; *J. Chem. Soc., Chem. Commun.* **1976**, 501.
(31) Titus, D. D.; Lee, J.-S.; Ziolo, R. F. *J. Organomet. Chem.* **1976**, *120*, 381.

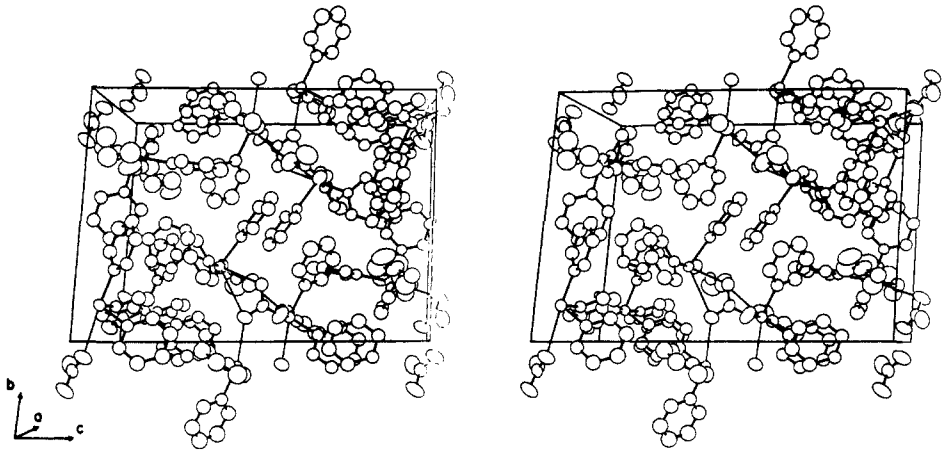

Figure 5. Overall view of the crystal packing in $Ph_3Te^+NO_3^-$.

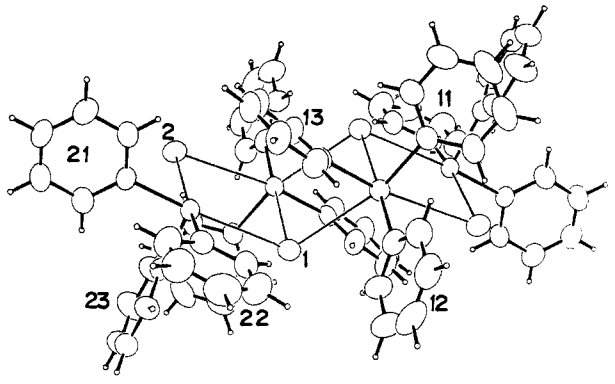

Figure 6. The tetrameric unit in $Ph_3Te^+Cl^-\cdot{}^1/_2CHCl_3$.

all the present S–O bond lengths (average 1.472 Å) have been lengthened by secondary/hydrogen bonding interactions and are thus much longer than the dimensions of the sulfate anions in the above trimethylsulfonium salt (1.430 (8), 1.395 (14) Å, both ×2).[32] However, the present anion dimensions compare favorable to those observed in several inorganic sulfate salts such as $(TeF_3)_2SO_4$[6] [average S–O = 1.468 Å] and $Na_2Te(OH)F_3(SO_4)$[33] [average S–O = 1.474 Å]. Deviations in the OSO angles in the anions in the present salt are slight [108.0 (6)–111.0 (5)°].

The Triphenyltelluronium Cations. In $Ph_3Te^+Cl^-\cdot{}^1/_2CHCl_3$, $Ph_3Te^+NO_3^-$, and $(Ph_3Te)_2SO_4\cdot 5H_2O$ it is possible to define the orientations of the phenyl rings of the cations by use of either the torsion angles involving the calculated (approximately tetrahedral, C–Te–1p angles are ~120–125°) lone pair positions and the ortho carbon atoms in the rings or the angles between the mean planes through the phenyl rings. By using the first method, the conformations of $Ph_3Te(1)^+$ and $Ph_3Te(2)^+$ in $Ph_3TeCl\cdot{}^1/_2CHCl_3$ may be approximately described as (85, 30, 30°) and (135, 140, 145°), respectively; those for Te(1–4) in Ph_3TeNO_3 as (170, 100, 10°), (35, 55, 35°), (30, 50, 20°), and (170, 100, 140°), respectively, and in $(Ph_3Te)_2SO_4\cdot 5H_2O$, Te(1–4) are described as (45, 10, 55°), (65, 10, 50°), (130, 120, 150°), and (130, 125, 170°). Alternatively, with use of the angles between the planes (n1)–(n2), (n1)–(n3), and (n2)–(n3) in each triplet then the conformations of the cations are as follows: $Ph_3TeCl\cdot{}^1/_2CHCl_3$, (50, 103, 33°) and (92, 82, 93°); Ph_3TeNO_3, (63, 113, 130°), (80, 96, 106°), (88, 101, 116°), and (68, 92, 58°), and in $(Ph_3Te)_2SO_4\cdot 5H_2O$, (129, 87, 80°), (72, 101, 64°), (95, 77, 72°), and (77, 121, 83°). Furthermore, in the crystal packings of these three compounds several examples of near parallelism between the phenyl rings of different cations and other situations where adjacent rings are near 90° to each other occur.[34]

(32) Yu, P.-Y.; Mak, T. C. W. *Z. Krist.* **1978**, *147*, 319.
(33) Gorbunova, Y. E.; Linde, S. A.; Pakhomov, V. I.; Kokunov, Y. V.; Gustyakova, M. P.; Buslaev, Y. A. *Koord. Khim.* **1983**, *9*, 524.

Of note in the present examples and Ph_3Te^+ salts in general is the wide range of C–Te–C bond angles observed [90.6–100.1° (Table III, supplementary material)]. Even average bond angles are found to vary significantly from 94.1 to 97.0° and many of these values are comparable to average bond angles for some trimethyltelluronium salts (Table VII, supplementary material). Trends in these bond angles with, for example, C–Te–C decreasing with increasing (shortening) Te···Cl secondary bonding are not readily apparent presumably due to other packing forces, noteably interactions between phenyl rings.[34,35] Similarly Te–C distances are determined with varying accuracies preventing any observation of the effects of the secondary bonds on primary bond lengths. Additionally in the Ph_3Te^+ cations, changes in the internal bonding of the phenyl rings and particularly their orientations with respect to the Te–C bonds are observed to be quite variable in extent.[35] However, the average CTeC (C = alkyl, aryl) bond angles are always smaller than corresponding average CSeC angles in analogous salts (Table IV, supplementary material) consistent with the stronger secondary interactions in the Te compounds. Finally, secondary bonding in sulfonium salts is even weaker and the CSC bond angles are slightly larger than their Se counterparts (cf. the discussion of secondary bonding in the corresponding group 16 trihalide cations[6]).

Discussion of Solid-State NMR Spectra

(a) The Me_3Te^+ Cation. The solid-state ^{125}Te NMR spectra of Me_3TeNO_3 as both a static powder and with MAS are given

(34) Angles between the mean planes of the phenyl rings are the following (deg): [n – 21, 22, 23] = (33, 92, 115) [n = 11], (83, 94, 163) [n = 12] and (95, 16, 78) [n = 13] for $Ph_3TeCl\cdot{}^1/_2CHCl_3$; [$n$ – 21, 22, 23] = (76, 42, 118) [n = 11], (116, 37, 94) [n = 12] and (37, 105, 63) [n = 13] and [m – 41, 42, 43] = (55, 52, 109) [m = 31], (35, 95, 89) [m = 32] and (110, 52, 28) [m = 33] for Ph_3TeNO_3. In $(Ph_3Te)_2SO_4\cdot 5H_2O$ some interring angles in the polymeric chain are the following (deg): 5.1, 7.6, and 4.4 for (11 – 23, 31, 41) respectively, 7.4 for (12 – 43), 15.9, 5.1, and 10.0 for (13 – 21, 32, 42), respectively, 12.3, 10.5, 6.2, 8.9, 11.9, and 13.0 for (21 – 32), (22 – 33), (23 – 31), (23 – 41), (31 – 41), and (32 – 42), respectively.

(35) steric compression between the phenyl rings results in TeCC angles deviating significantly from 120° [116.6 (3) to 123.6 (3)° for $Ph_3TeCl\cdot{}^1/_2CHCl_3$, 116.0 (4) to 124.5 (4)° for Ph_3TeNO_3, and 112.5 (9) to 124.3 (10)° for $(Ph_3Te)_2SO_4\cdot 5H_2O$] and for the Te atoms to deviate significantly from the plane of each ring [max Δ_{Te} = 0.216 Å for $Ph_3TeCl\cdot{}^1/_2CHCl_3$, 0.189 Å for Ph_3TeNO_3, and 0.129 Å for $(Ph_3Te)_2SO_4.5H_2O$]. Internal CCC angles then range from 117.7 (6) to 122.0 (4)° with C(1–2–3) and C(5–6–1) generally less than 120° (Supplementary Tables C and D). In $Ph_3TeCl\cdot{}^1/_2CHCl_3$ the largest Δ_{Te} is for ring **13** which is involved in the short Te(2)···Ph interactions mentioned above while Δ_{Te} for ring **12** is only ~0.002 Å, but the TeCC angle for this ring differs the most from 120° [116.6 and 123.6 (3)°]. In Ph_3TeNO_3 the rings involved in the shortest Te···Ph contacts [(**13**) and (**33**)] have quite modest Δ_{Te} values (0.057 and 0.047 Å) but significantly different TeCC angles, the largest CTeC angle (99.4°) involves two rings with the smallest Δ_{Te} values while the smallest CTeC angle (92.5°) involves the rings with the largest Δ_{Te} values (0.189 and 0.101 Å). Similarly there appears to be no systematic trend between the CTeC or TeCC angles and Δ_{Te} values for $(Ph_3Te)_2SO_4\cdot 5H_2O$, except to note that the largest Δ_{Te} values are generally associated with the most unsymmetrical TeCC angles [ring **41** is an exception, however]. The two largest CTeC bond angles (100.1 and 99.2°) are associated with Ph rings with large and small Δ_{Te} values [**11** and **13**] and two small Δ_{Te} values [**41** and **43**].

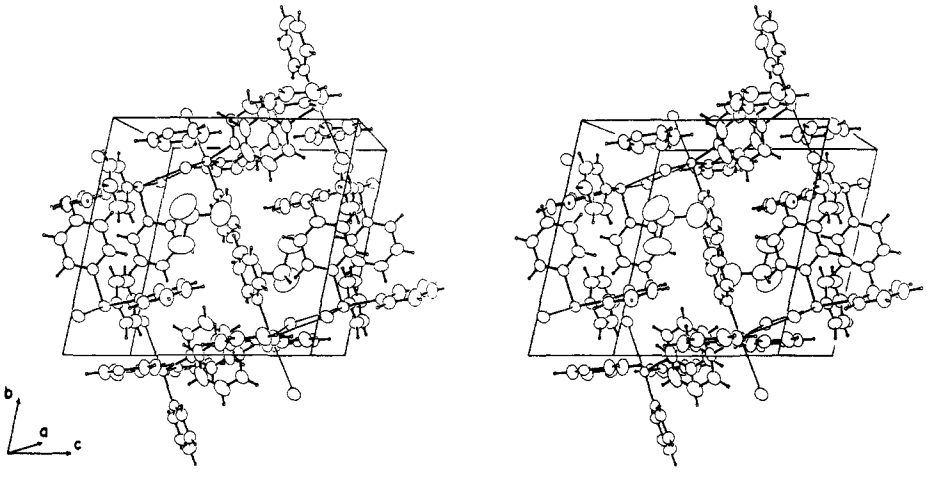

Figure 7. Overall view of the crystal packing in $Ph_3Te^+Cl^-\cdot{}^1/_2CHCl_3$.

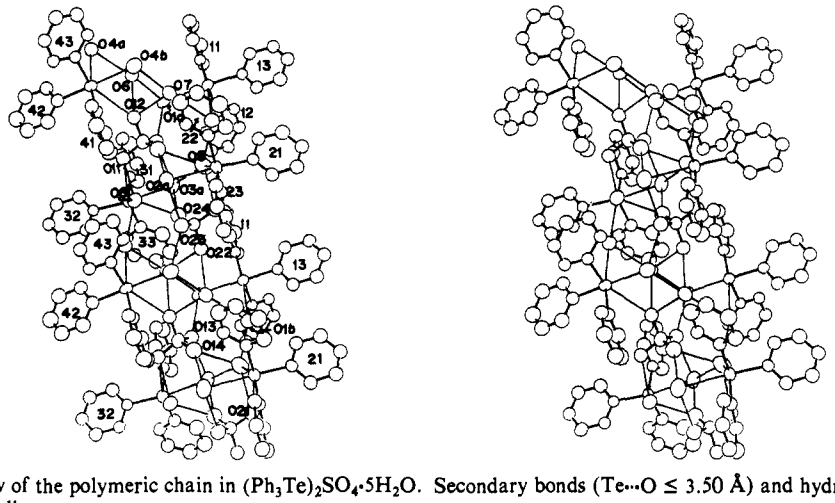

Figure 8. Stereoscopic view of the polymeric chain in $(Ph_3Te)_2SO_4\cdot 5H_2O$. Secondary bonds (Te···O ≤ 3.50 Å) and hydrogen bonds (O···O distances ≤3.15 Å) indicated as thin lines.

in Figure 9. The static powder pattern is only 110 ppm wide, which is similar to that of telluric acid.[8] In comparison, the shielding tensor for frozen Me_2Te is over 1200 ppm wide.[8] This suggests that the Te environment in Me_3TeNO_3 may have pseudooctahedral symmetry as is the case for telluric acid, $Te(OH)_6$. In addition, the Me_3TeNO_3 powder pattern has nearly axial symmetry and suggests that the C_{3v} symmetry of the isolated cation is approximately maintained in the Me_3TeNO_3 structure. This, of course, is consistent with the crystal structure determination, which shows three interactions between tellurium and oxygen atoms of the nitrate anions to give a distorted octahedral arrangement about Te (Figure 3). The C–Te–C angles, Te–C bond lengths, and Te···O secondary bond lengths are fairly uniform and are consistent with the nearly axial ^{125}Te shielding tensor (see Table III, supplementary material). The ^{125}Te MAS spectrum of Me_3TeNO_3 consists of a single resonance at the isotropic shift plus spinning side bands and is consistent with the single unique crystallographic Te site in the structure (Figure 9), while the ^{13}C MAS spectrum of Me_3TeNO_3 contains only a single resonance (Table VIII, supplementary material). Although the three methyl groups are not crystallographically equivalent, they are sufficiently similar that individual resonances were not resolved.

Like that of Me_3TeNO_3, the static ^{125}Te spectrum of $Me_3TeCl\cdot H_2O$ is about 110 ppm in width and is consistent with the pseudooctahedral Te environment established by the crystal-structure determination. The powder pattern is not axially symmetric, indicating that the symmetry at Te is, however, not exactly C_{3v} (cf. Table VII (supplementary material) and Figure 10a).

The ^{125}Te MAS spectrum of $Me_3TeCl\cdot H_2O$ consists of a septet at the isotropic shift plus spinning side bands (Figure 10a). Since Cl has a spin of $^3/_2$, the septet suggests coupling to two equivalent

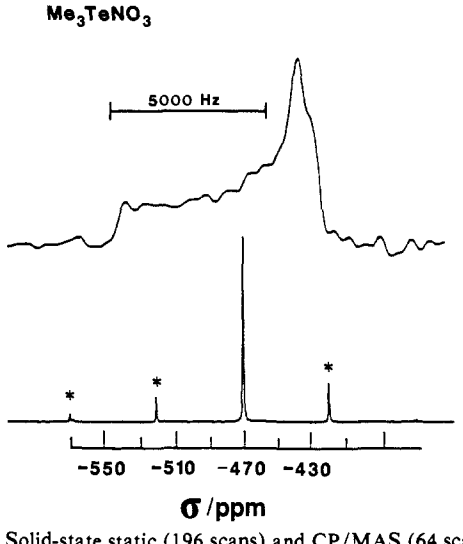

Figure 9. Solid-state static (196 scans) and CP/MAS (64 scans) ^{125}Te NMR spectra for $Me_3Te^+NO_3^-$. An asterisk indicates spinning side bands.

Cl atoms. In the structure determination these two Cl atoms are crystallographically equivalent due to the mirror plane through the Me_3Te^+ cation. Couplings of spin $^1/_2$ nuclei to quadrupolar nuclei have been observed before in the solid state, for example, coupling to ^{14}N in ^{13}C spectra,[36] and coupling to ^{63}Cu in ^{31}P

(36) Zumbulyadis, N.; Henrichs, P. M.; Young, R. H. *J. Chem. Phys.* **1981**, *75*, 1603.

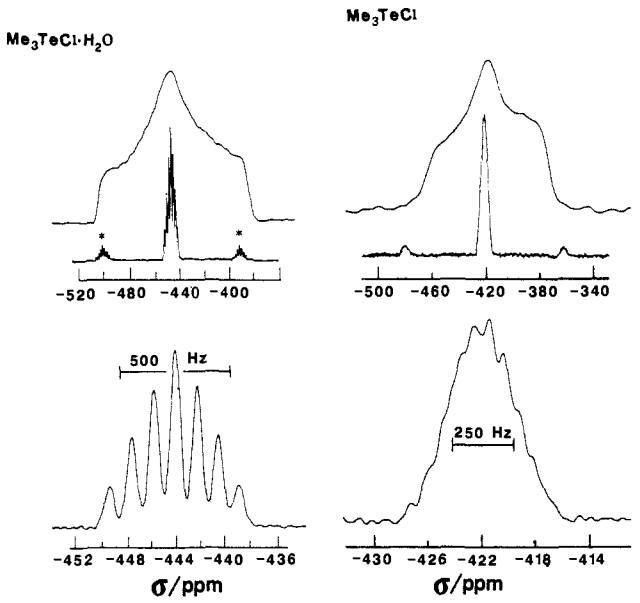

Figure 10. Solid-state static and CP/MAS ^{125}Te NMR spectra for (a) $Me_3Te^+Cl^-\cdot H_2O$ (static, 1212; MAS, 240 scans) and (b) $Me_3Te^+Cl^-$ (static, 6400, MAS, 240 scans). An asterisk indicates spinning side bands.

spectra.[37] Generally, distorted multiplets arise as a result of dipolar contributions to the coupling. For $Me_3TeCl\cdot H_2O$, a symmetric pattern was obtained, indicating purely J coupling. The lack of a dipolar contribution is consistent with the long Te···Cl distance and /or a small Cl quadrupole coupling constant.

The intensities of the septet components depart slightly from the ideal 1:2:3:4:3:2:1 ratio as the ^{35}Cl and ^{37}Cl nuclei, with natural abundances of 75.4 and 24.6%, respectively, have slightly different coupling constants. This causes the multiplet line width to increase progressively on going from the central component to the outer components (Figure 10a). By assuming that the observed splitting is a weighted average of the two isotopes, the ^{125}Te–^{35}Cl coupling is calculated to be 106 ± 5 Hz.

The ^{13}C MAS spectrum of $Me_3TeCl\cdot H_2O$ identifies two distinct methyl environments in a 2:1 ratio (Table VIII, supplementary material) as expected from the crystal structure since two methyl groups and two secondary bonded Cl atoms are symmetry related by reflection in a mirror plane that includes the Te atom and the third methyl group (Figure 1). There is a third secondary bond from the oxygen atom of the water molecule to Te, so that the symmetry about Te is still AX_3Y_3E. The asymmetry in the secondary bonding environment, however, results in a significant variation in the C–Te–C angles (Table VII, supplementary material) and this is reflected in the general shape of the powder pattern in the ^{125}Te NMR spectrum.

The ^{13}C CP/MAS spectrum of Me_3TeCl (Table VIII, supplementary material) identifies three distinct methyl groups. The ^{125}Te static spectrum (Figure 10b) is very narrow, suggesting that the Te atom in anhydrous Me_3TeCl has an AX_3Y_3E geometry with three distinct Te–Cl interactions opposite these methyl groups and three different ^{125}Te–Cl couplings. If the three Cl atoms were equivalent, a 1:3:6:10:12:12:10:6:3:1 decet would be anticipated in the ^{125}Te MAS spectrum (ignoring isotope effects). Indeed the observed spectrum is not inconsistent with such an interpretation, implying that the Te–Cl couplings are all approximately 65 Hz. This is not as large as the coupling for the monohydrate, perhaps indicating a somewhat larger Te–Cl distance in the anhydrous form, as would be expected from bond valence arguments if the Cl^- ion is expected to form 3 Te···Cl secondary bonds as opposed to the two interactions in the hydrate [Cf: the Te···Cl distances in the dimeric units in unsolvated Ph_3TeCl with the corresponding Te···Cl distances for the tetrameric unit in $Ph_3TeCl\cdot{}^1/_2CHCl_3$ (Table III, supplementary material)].

(37) Menger, E. M.; Veeman, W. S. *J. Magn. Reson.* **1982**, *46*, 257.

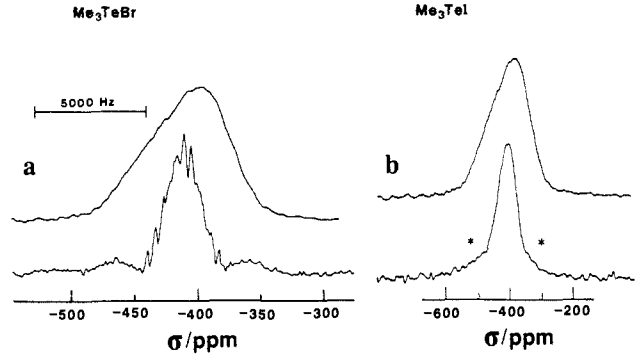

Figure 11. Solid-state static and CP/MAS ^{125}Te NMR spectra for (a) $Me_3Te^+Br^-$ (static, 2192; MAS, 2608 scans) and (b) $Me_3Te^+I^-$ (static, 2580; MAS, 176 scans). An asterisk indicates spinning side bands.

The inequivalence of the methyl and Cl neighbors about Te is reflected in the general powder pattern observed in the static ^{125}Te NMR spectrum (Figure 10b). The line shape is somewhat narrower than that of the monohydrate, however, reflecting the increased symmetry of 3 Cl neighbors compared with 2 Cl atoms and 1 O atom found in the monohydrate.

Coupling to Br causes severe distortion in the ^{125}Te static spectrum of Me_3TeBr and only one of the three shielding tensor elements can be read directly from the plot (Figure 11a). The other two elements were estimated from the isotropic shift and the half-width of the ^{125}Te-Br multiplet, which were extracted from the MAS spectrum (Table VIII). The narrow powder pattern again suggests a distorted octahedral environment for Te in Me_3TeBr.

Some fine structure resulting from ^{125}Te–Br coupling is observed in the ^{125}Te MAS spectrum of Me_3TeBr (Figure 11a). The magnitude of the coupling is considerably larger than the ^{125}Te–Cl couplings observed in Me_3TeCl and $Me_3TeCl\cdot H_2O$, but the resolution is better in the chlorides. The complex nature of the Me_3TeBr multiplet may result from crystallographic inequivalence of Br and/or Te atoms, or a contribution from dipolar and scalar coupling. The ^{13}C MAS spectrum of Me_3TeBr, however, demonstrates that there are only two distinct types of methyl group, in a ratio of 2:1 (Table VIII, supplementary material). It is unlikely, therefore, that there are crystallographically inequivalent Te atoms in the structure. The two distinct methyl resonances in the ^{13}C spectrum could result from one of several secondary bonding environments, provided that approximate mirror symmetry is maintained. The complexity of the multiplet observed in the ^{125}Te MAS spectrum and the narrow powder pattern, however, rule out AX_3YE and AX_3Y_2E environments. A structure similar to Me_3TeI is likely, where the Te atoms are linked into predominantly dimeric units by two bridging halide ions and each Te atom has an additional, somewhat longer interaction with a third halide ion (Figure 2). The unique resonance in the ^{13}C MAS spectrum would then result from the methyl group opposite this unique Te···Br interaction. Depending on the similarity of the two supposed bridging interactions, two or three different ^{125}Te–Br couplings would be expected. Dipolar and scalar contributions to the coupling result in considerable asymmetry in the ^{125}Te CP/MAS spectrum, however, and it is not possible to resolve the individual ^{125}Te–Br coupling constants. If the multiplet results from coupling to three Br atoms, the mean ^{125}Te–Br coupling is one-ninth of the separation of the outermost lines, that is, 350 Hz.

The ^{125}Te CP/MAS spectrum of Me_3TeI is nearly as broad as the static line shape (Figure 11b). It would appear that the dipolar and scalar interactions are considerably more important here than for X = Cl or Br, and no ^{125}Te–^{127}I couplings are resolved in the MAS spectrum. The shape of the powder pattern is strongly distorted by this coupling, but the overall width is still ca. 100 ppm, consistent with the distorted octahedral environment for Te established by the crystal structure determination. Two distinct methyl resonances were observed in the ^{13}C MAS spectrum of Me_3TeI (Table VIII, supplementary material), suggesting a

mirror plane in the structure, as was the case for $Me_3TeCl{\cdot}H_2O$. The crystal structure of Me_3TeI did not reveal such a plane, although the crystal packing (Figure 2) indicates that the environments of C(1) and C(2) are very similar and significantly different from that of C(3). A far less severe broadening of the NMR line shapes is observed in the static and MAS ^{77}Se NMR spectra of Me_3SeI.[38] This reflects the considerably weaker Se···I interaction in Me_3SeI compared to the three relatively strong Te···I interactions in Me_3TeI (Tables III and IV, supplementary material).

One of the ^{125}Te chemical shift tensor elements for an isolated Me_3Te^+ cation likely lies along the 3-fold axis of the cation. In the cation of Me_3TeNO_3, the Te atom retains approximate 3-fold symmetry in the crystal structure and a nearly axial powder pattern results (Figure 9). The unique tensor element, σ_{zz}, lies to low field of σ_{xx} and σ_{yy}, that is, the 3-fold axis of the cation is deshielded with respect to the plane perpendicular to this axis. The chemical shift tensors of Me_3TeBr and Me_3TeI are not very much different from axial, and again the z axis is deshielded (Figure 11). A similar situation is found for the ^{77}Se shielding tensor in Me_3SeI.[38]

The ^{125}Te isotropic shifts for Me_3TeX (X = Cl, Br, or I) follow a simple trend with a high-field shift (increased shielding of the Te nucleus) correlating with an increase in the size and electropositive nature of X, that is, an increase in the anticipated strength of the Te···X secondary bonding (Table VIII, supplementary material).

(b) The Ph_3Te^+ Cation. The ^{125}Te NMR spectra of the Ph_3Te^+ compounds were considerably more difficult to obtain than those of the corresponding Me_3Te^+ compounds due to the following: (1) The mass of the Ph_3Te^+ cation is more than double the mass of the Me_3Te_+ cation, so fewer ^{125}Te nuclei are being sampled. (2) There are frequently 2 or more crystallographically distinct Te sites in the Ph_3Te^+ structures, further diluting the individual Te nuclei. (3) The spin–lattice relaxation time of a phenyl proton is in general considerably longer than that of a methyl proton and the distance between the phenyl protons and the tellurium nuclei in Ph_3Te^+ is greater than the distance between the methyl protons and the tellurium nuclei in Me_3Te^+, so that cross-polarization is less efficient for phenyl substituents. (4) The ^{125}Te chemical shift tensors of the Ph_3Te^+ compounds are somewhat broader than those of the Me_3Te^+ compounds. As a result, only CP/MAS spectra were recorded for the triphenyltelluronium compounds. The chemical shift tensor widths could be estimated from the MAS spectra and ranged from approximately 220 ppm in Ph_3TeCl to 320 ppm in Ph_3TeNO_3.

In the case of Ph_3TeNO_3, the 4 crystallographically independent tellurium nuclei were resolved in the MAS spectrum (Table VIII, supplementary material). The large range of chemical shifts observed for these four nuclei, 26 ppm, reflects the substantial differences in their secondary bonding environments (see above). In $Ph_3TeCl{\cdot}{}^1/_2CHCl_3$ there are two Te environments, one with two Te···Cl interactions and the other with three. There is a 31-ppm difference in the ^{125}Te chemical shifts of these two environments (Table VIII, supplementary material). Although there are two crystallographically distinct Te nuclei in Ph_3TeCl,[2] there is very little difference in their environments and a single resonance is observed in the MAS spectrum (Table VIII, supplementary material).

It was anticipated that there would be a substantial chemical shift difference between Ph_3TeCl, where the Te atoms have only two secondary bonds to chlorine, and $(Ph_3Te)_2Hg_2Cl_6$, where the unique Te atom takes part in three Te···Cl secondary bonds,[9] but very little difference was observed (Table VIII, supplementary material). Interactions of the two independent Te atoms in Ph_3TeCl with phenyl substituents from adjacent cations (both Te atoms are in good position for a face-on interaction with a nearby phenyl ring) presumably compensate for the missing chlorine atom. Furthermore, although there are 3 Te···Cl interactions in $(Ph_3Te)_2Hg_2Cl_6$ these are considerably weaker (av 3.467 Å) than the 2 Te···Cl interactions in Ph_3TeCl (av 3.204 Å). The contribution of the secondary bonding to the shielding of the Te nuclei in these compounds is apparently equivalent and their isotropic chemical shifts are nearly identical. In $Ph_3TeCl{\cdot}{}^1/_2CHCl_3$ the environment Te(2) with only two Te···Cl interactions also forms a longer Te···Ph interaction. This environment probably corresponds to the resonance at 762 ppm in the CP/MAS spectrum of $Ph_3TeCl{\cdot}{}^1/_2CHCl_3$, that is, in close proximity to the resonances observed for Ph_3TeCl and $(Ph_3Te)_2Hg_2Cl_6$. The remaining resonance, at 731 ppm, probably corresponds to Te(1), the AX_3Y_3E environment. The Te···Cl interactions here (av 3.391 Å) are considerably stronger than those of the AX_3Y_3E enviromment of $(Ph_3Te)_2Hg_2Cl_6$. The 31-ppm shift to high field for Te(1) of $Ph_3TeCl.{}^1/_2CHCl_3$, therefore, is consistent with the greater shielding of the Te(1) nucleus in $Ph_3TeCl{\cdot}{}^1/_2CHCl_3$ as a result of stronger Te···Cl secondary interactions.

Similarly, the low-field resonances for Ph_3TeNO_3, at 802 and 793 ppm, probably result from Te(2) and Te(4), the environments with Te···Ph contacts, while the high-field resonances, at 786 and 776 ppm, probably result from Te(1) and Te(3), the environments with 3 or more Te···O interactions. As was the case for the Me_3Te^+ compounds, the isotropic shifts for Ph_3TeNO_3 are shifted to low field of the isotropic shifts for the Ph_3Te^+ compounds with chloro anions, reflecting the stronger secondary bonds formed between Te and chlorine compared with oxygen atoms of the nitrate ions.

Conclusions

The crystal structures and the solid-state ^{125}Te NMR spectra for a series of Me_3Te^+ and Ph_3Te^+ salts have been obtained. Whereas aqueous solutions of these compounds give narrow, featureless lines and the spectrum of an aqueous solution of R_3TeCl would be indistinguishable from that of R_3TeNO_3, for example, the solid-state spectra of these same compounds are markedly different and provide a wealth of information. Subtle changes in the cation geometry imposed by interactions with different anions and the extended environment of the Te nucleus (e.g., AX_3Y_3E or AX_3Y_2E) can be deduced from the ^{125}Te chemical shift tensors, isotropic chemical shifts, and, in some cases, couplings to neighboring nuclei. These ^{125}Te–halogen couplings are definitive proof of covalent interactions, that is, weak secondary bonds between the "anions" and "cations" in these compounds.

Acknowledgment. D. W. Davidson, now deceased, is thanked for providing the stimulating and supportive environment necessary for the NMR studies. The Natural Sciences and Engineering Research Council of Canada is thanked for providing an equipment grant for the diffractometer.

Supplementary Material Available: Tables of hydrogen atom positions, anisotropic thermal parameters, bond lengths and bond angles in the phenyl rings, equations of least-squares mean planes, and final structure factor amplitudes for compounds **1–6** (22 pages). Ordering information is given on any current masthead page.

(38) Collins, M. J.; Ratcliffe, C. I.; Ripmeester, J. A. *J. Magn. Reson.* **1986**, *68*, 172.